A Novel Air-gap Formation Method for Metal Interconnect

Youngjoon Choi, Sungsik Cho, Philoptics Co. Ltd.

Abstract— Electrospinning technology was introduced to the formation of air-gap in metal interconnection. A polyimide fiber-cluster layer was made with this technology on the line and space (L/S) patterns. After hot melting of the layer, a full air-gap structure was created.

I. INTRODUCTION

In the semiconductor technology roadmap, one of the most difficult interconnects challenges is the introduction of new materials that reduce dielectric permittivity [1]. Air has the lowest k-value material in the world. Its k-value is 1.00059 where vacuum is defined as 1.0 [2]. As mentioned in many earlier pieces of research, the air-gap interconnect structure is the ultimate solution but it is one of the most significant challenges in the manufacture of semiconductor devices at highly tight pitch technology nodes in the future [3-5].

This paper introduces a new air-gap formation method using electrospinning (E/S) [6-9]. It is different from the non-conformal CVD [10-13], and the sacrificial layer method [10, 14-19]. A polyimide nano-fiber-cluster layer (PI-nFCL) formed by E/S is changed into a dense polyimide (PI) film. Then it looks like a bridge on the patterns showing a perfect air-gap-like space.

II. EXPERIMENTAL

In this experiment, we utilized a single vertical nozzle type E/S machine and a varnish type polyimide (PI) for the E/S material among several polymer candidates [20-21]. The varnish has 18.9% of solid content in weight of PI with 25,000 mean molecular weight in N,N-dimethylacetamide solvent. We applied 0.05mm of inner diameter nozzle for E/S. The E/S parameters were 15.5kV of voltage on the metallic nozzle, -2.5kV on collector, 13.5cm of working distance, 25 micro-liter per minute of injection rate, room temperature (RT), and 45~50 % of relative humidity. We conducted 15-minutes of E/S on a 1cm x 1cm wafer specimen which has various aspect ratios of line and space (L/S) patterns as shown in Fig. 1-a.

After completion of E/S, the specimen was baked on a hot plate at 350°C for 2 minutes. The PI film was slightly etched by inductively coupled plasma-reactive ion etch (ICP-RIE) for 90 seconds under the conditions of O2/40sccm, Ar/10sccm, 20 mTorr at 400W. Then we deposited SiO2 on the RIE treated PI film with plasma-enhanced chemical vapor deposition (PECVD) for 30 minutes in the 80°C, 450 mTorr, at 300W,

¹Youngjoon Choi. Author in Philoptics Co. Ltd. 19-1 Jigotjoongang-ro, Osan City, Gyeong-gi-do, S. Korea (corresponding author, e-mail: luxhi@naver.com)

Sungsik Cho. Author in Philoptics Co. Ltd. (e-mail: ssjo@philoptics.com)

applying SiH4(9sccm)/N2O(25sccm) as shown in Fig. 1-b.

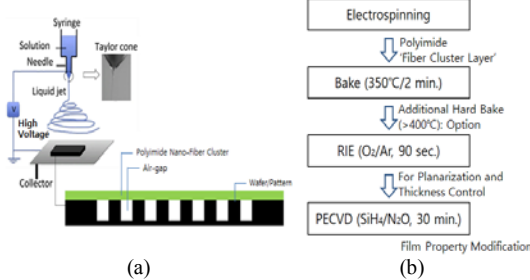


Fig. 1. (a) Electrospinning air-gap formation scheme (b) Full process.

We observed the top and vertical views of the results for each process step with SEM. We measured the glass point (Tg) and decomposition point (Td) of the PI with TG-DTA. We also measured the hardness and Young's modulus of the hard-baked PI/SiO2 complex layer with ZwickRoell Nanoindent machine.

We did a k-value simulation for this air-gap. The simulation conditions were as follows: Cu/Air-gap structure, 10 to 50nm of half-pitch of line and space by 10nm width increasing, TaN/Ta liner, and so on. More detailed conditions are summarized in TABLE I in section III, "RESULTS AND DISCUSSION". The I-V curve of the PI/SiO₂ complex layer was also estimated.

III. RESULTS AND DISCUSSION

The PI-nFCL is shown in Fig. 2. The diameter of the PI fiber was approximately 150 nm to 300 nm $3\mu m$. The PI-nFCL on the patterns left space, air-gap, between the line patterns.

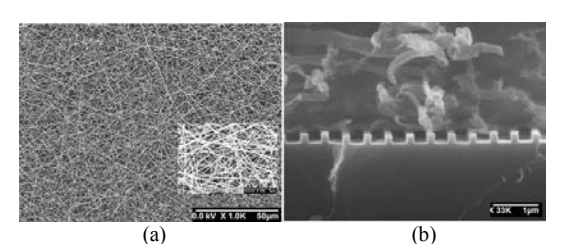


Fig. 2. PI varnish E/S results. (a) Top view (x1,000), inset picture (x10,000) (b) Cross section view. PI-nFCL is about 3 μm-thick.

The PI-nFCL changed from fibrous pored cluster film to completely sealed film after baking on a hot plate at 350 °C for two minutes (Fig. 3). Around 3 μ m-thick PI-nFCL was transformed to approximately 300 nm-thick dense PI film.

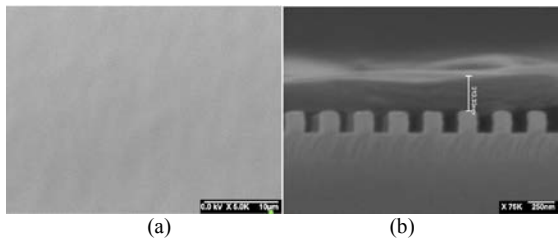


Fig. 3. A dense PI film formation after 350°C of hot plate bake for 2 minutes. (a) Top view (b) Cross section view (thickness of the PI film

After RIE followed by SiO₂ PECVD on the dense PI, the observed surface was translucent and relatively uniform. Patterns underneath the film were visible (Fig. 4-a). Partial silylation and/or oxidation of the PI film by PECVD may be the reason. A maximized volume of air-gap formation is shown in Fig. 4-b.

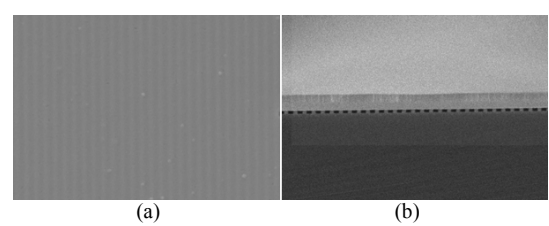


Fig. 4. After RIE and SiO₂ PECVD (a) Top view (translucent) (b) Cross section view (relatively uniform than PI film surface)

The air-gaps in various aspect ratios (A/R) are shown in Fig. 5. A rectangular air-gap was formed up to at least 3.4:1 of A/R (6-a \sim 6-c). Sagging was observed at 7:1(Fig. 6-d), 12:1(Fig. 6-e), and 26:1(Fig. 6-f). We can say that desired air-gap may not be formed above a certain value of A/R. And on closer observation, it seems that there is slight interlocking between the PI layer and pattern.

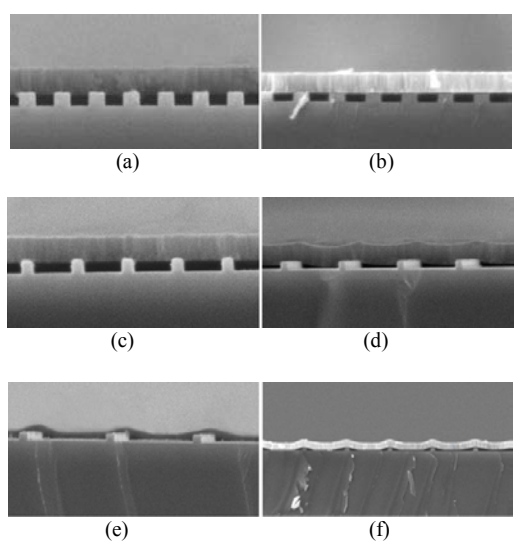


Fig. 5. Air-gap formation in various A/R (a) 1.2:1 (b) 2.4:1 (c) 3.4:1, (d) 7:1 (e) 12:1, (f) 25.9:1. Upon closer look, interlocking between PI film and pattern is observed. In A/R 7:1, 12:1 and 25.9:1, sagging of the PI films exist

Comparison between air-gap formation in the pattern area and simple deposition at the blank area is shown in Fig. 6

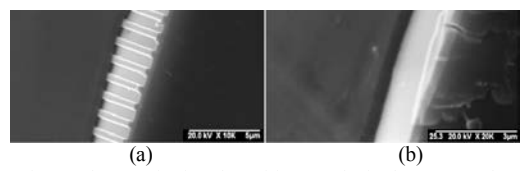


Fig. 6. Electrospinning deposition results in the patterned area and the blank area. (a) Pattern area (b) Blank area

The effect of hard baking, 450°C/Hot Plate/5 minutes, is shown in Fig.7. Shrinkage of the air void at the step was observed but there was no noticeable difference in the air-gap shape. Additional higher temperature baking may bring a positive effect in adhesion and film conformity to the substrate.

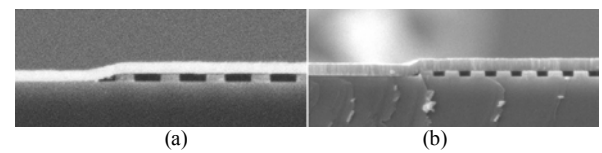


Fig. 7. Hard bake effect evaluation (a) Apply the first bake only (350°C/2 min.) (b) Additional high temperature bake (450°C/5 min.). After hard bake the step coverage was improved.

According to the TG-DTA result of PI-nFCL, the glass point was 330°C, and serious decomposition starts to take place about 480°C (Fig. 8).

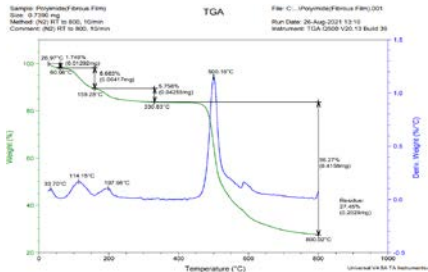


Fig. 8. TG-DTA of PI-nFCL. Volitiles, moisture, and solvents evaporate under 200°C. Tg is 330°C and Td is about 480°C.

The Vicker's hardness of the PI/SiO₂ complex film was 1445.4 kp/mm by. Young's modulus was 183.6Gpa. The hardness and Young's modulus of the complex film were estimated as 67.2%, and 82.9% of those of the reference PECVD SiO₂ film respectively.

The conceptual structure of Cu/air-gap according to this E/S air-gap formation method is shown in Fig. 9. The inputs for the k-value simulation are in Table I.

According to our simulation, k-values were 1.43, 1.43, 1.52, 1.57, and 1.67 for 50nm, 40nm, 30nm, 20nm, and 10nm half pitches of the copper lines, respectively. They are summarized in Fig. 10. and the inset table. These results are similar to the k-values of the ideal air-gap structures, around $1.5 \sim 1.7$, in V. Kumaresan and his colleagues' work [22].

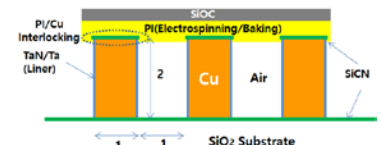


Fig. 9. Conceptual structure of the Cu/Air-gap

TABLE I Inputs for k-value simulation SiO2

Cu Wire Half Pitch (nm)	10, 20, 30, 40, 50 (1:1 Line and Space)
Height of Cu Wire	Twice of the Wire Width
Cu Liner	TaN/Ta
Liner Thickness (nm)	1.5
PI Interlocking to Cu Wire	5% of the Cu Wire Height
k-value of Materials	SiO2(3.9), SiCN(4.81), SiOC(3.04), PI(3.1)

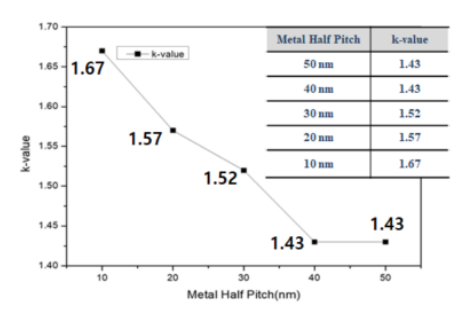


Fig. 10. Simulated k-values for various metals half pitch

I-V curve of the PI/SiO2 complex layer is shown in Fig. 11. The breakdown voltage (BV) was estimated to be in the range of $10\sim15$ MV/cm

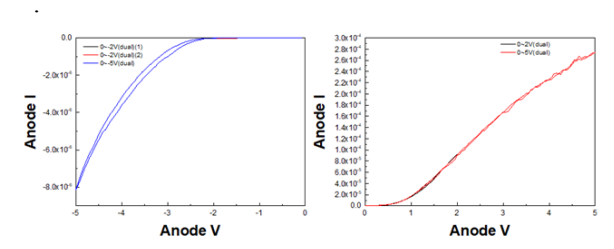


Fig. 11. I-V Curve of the PI/SiO2 complex layer. -5V \sim +5V, BV appears to be in the range of $10\sim15$ MV/cm.

Table II is a summary of the air-gap property in terms of thermal, mechanical, and electrical aspects

Table II Summary of the E/S air-gap properties

k-value		~1.5
Thermal Property	Tg(Glass Temperature)	350°C
	Tg after PECVD	>450°C
	Td(Decomposition Temperature)	~450°C
	CTE(Coefficient of Thermal	~10 ppm/°C
	Expansion)*	
Hardness		1445.4 kp/mm²
Elasticity(Young's Modulus)		183.6 GPa
Adhesion to Cu**		Good
Breakdown Voltage		10~15 MV/cm

^{*} CTE is a given data from polyimide manufacture

IV. CONCLUSION

In this experiment, we demonstrated a novel air-gap formation scheme using polyimide electrospinning technology. There will be better electrospinning conditions and many other prospective material candidates. We have to do a more intensive material study and process improvement to apply it to mass production.

REFERENCES

- [1] International Roadmap for Devices and Systems 2017 Edition,
- [2] Wikipedia, Available at: Relative permittivity Wikipedia
- [3] International Technology Roadmap for Semiconductors 2.0, 2015 Edition, Interconnect. Available at: http://public.itrs.net
- [4] P. Besser, "BEOL Interconnect Innovations for Improving Performance", NCCAVS Symposium at San Jose, CA, 2017.
- [5] M. Baklanov. "Challenges in implementation of low-k dielectrics in advanced ULSI interconnects" Nano and Giga Challenges at Tomsk, Russia, 2017.
- [6] R. Stoddard, X. Chen, "Electrospinning of ultra-thin nanofibers achieved through comprehensive statistical study" Material Research Express 3, 2016, 055022
- [7] A. Haider, S. Haider, I.K Kang, "A Comprehensive review summarizing the effect of electrospinning parameters and potential applications of nanofibers in biomedical and biotechnology", Arabian Journal of Chemistry, 2015
- [8] Karakas H. "Electrospinning of nanofibers and their applications", 2014, MDT Electrospinning 3, pp. 1-35
- [9] Chaobo Huang et al., "Electrospun polymer nanofibers with small diameters" Nanotechnology 17, 2006, pp. 1558-1563
- [10] L.G. Gosset et al., "Advanced Cu interconnects using air gaps", Microelectronic Engineering 82, 2005, pp. 321-332
- [11] J. Noguchi, et al., IEEE Trans. Electron Devices 53(3), 2005, pp. 352-358
- [12] S. Nitta, et al., "A multilevel copper/low-k/airgap BEOL technology, Advanced Metallization Conference, 2008, pp. 329-336
- [13] T Ueda, et al., "Extremely Low Keff.(1.9) Cu Interconnects with Air Gap Formed Using SiOC", IITC 2007, pp. 141-143
- [14] R. Daamen, et al., International Interconnect Technology Conference, 2007, pp. 61-63
- [15] F. Gaillard, et al., "Chemical etching solutions for air gap formation using sacrificial oxide/polymer approach" Microelectronic Engineering, Vol. 83, 2006, 2309-2313
- [16] M. Pantouvaki, et al., "Air gap formation by UV-assisted decomposition of CVD material" Microelectronic Engineering, Vol. 85, 2008, 2071-2074
- [17] R. Daamen, et al., "Multi-Level Air Gap Integration for 32/22 nm nodes using a Spin-on Thermal degradable Polymer and a SiOC CVD Hard Mask" International Interconnect Technology Conference, 2007, pp. 61-63
- [18] R. Gras, et al., "Multi levels Air Gap Integration using Sacrificial Material Approach for Advanced Cu Interconnect Technologies", International Interconnect Technology Conference, 2008, 4546965
- [19] N. Nakamura, et al., "Cost-effective air-gap interconnects by all-in-one post-removing process" International Interconnect Technology Conference, 2008, pp. 193-195
- [20] S. Kohse, N. Grabow, K. Peter et al., "Electrospinning of polyimide nanofibers-effects of working parameters on morphology", Current Directions in Biomedical Engineering 2017 3(2): 687-690
- [21] Wikipedia, Available at: http://en.wikipedia.org/wiki/polyimide
- [22] V. Kumaresan, et al., "Simulation and measurement of the capacitance benefit of air gap interconnects for advanced technology nodes" Microelectronic Engineering 120, 2014, pp. 90-94

^{**} Qualitative estimation from a trial test on PVD Cu layer